

# RSC Advances



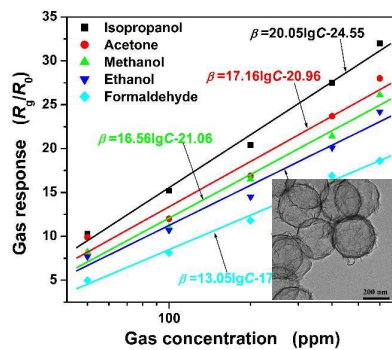
This is an *Accepted Manuscript*, which has been through the Royal Society of Chemistry peer review process and has been accepted for publication.

*Accepted Manuscripts* are published online shortly after acceptance, before technical editing, formatting and proof reading. Using this free service, authors can make their results available to the community, in citable form, before we publish the edited article. This *Accepted Manuscript* will be replaced by the edited, formatted and paginated article as soon as this is available.

You can find more information about *Accepted Manuscripts* in the [Information for Authors](#).

Please note that technical editing may introduce minor changes to the text and/or graphics, which may alter content. The journal's standard [Terms & Conditions](#) and the [Ethical guidelines](#) still apply. In no event shall the Royal Society of Chemistry be held responsible for any errors or omissions in this *Accepted Manuscript* or any consequences arising from the use of any information it contains.

NiO hollow microspheres synthesized through SiO<sub>2</sub> spheres template-assisted approach show a very good gas response towards volatile organic compound vapors.





Journal Name

ARTICLE

Received 00th January 20xx,  
Accepted 00th January 20xx

DOI: 10.1039/x0xx00000x

www.rsc.org/

## NiO nanosheets assembled into hollow microspheres for highly sensitive and fast-responding VOCs sensor

Qing Li,<sup>a</sup> Nan Chen,<sup>a</sup> Xingxing Xin,<sup>a</sup> Xuechun Xiao,<sup>a,b</sup> Yude Wang<sup>\*a,b</sup> and Igor Djerdj<sup>\*c</sup>

Uniform NiO hollow microspheres constituted with nanosheets were synthesized by a simple water bath method through a SiO<sub>2</sub> spheres template-assisted approach and applied for an efficient gas sensor towards volatile organic compound vapors (VOCs). The structural characterizations reveal that sub-micrometer NiO hollow microspheres (350–400 nm) were formed assembling NiO nanosheets, which were composed of 20–40 nm thickness NiO sheets. The gas responses of the five reductive gases of isopropanol, acetone, methanol, ethanol and formaldehyde at a low concentration of 50 ppm are 11.3, 9.9, 8.2, 7.7 and 5.0, respectively. NiO hollow microspheres showed higher response for VOCs compared to other nanostructured NiO previously reported in literatures. The gas sensor based on NiO hollow microspheres shows a high response, fast response and recovery towards VOCs, making it promising candidate for practical detector of VOCs. Improved performance of NiO hollow microspheres was attributed to hollow spaces that offer a high surface-to-volume ratio and an intrinsically large specific surface area of 167.31 m<sup>2</sup>/g, leading to improved surface activities. It was suggested that oxygen adsorption over NiO surface resulted in the formation of absorbed oxygen layer, which possibly decrease in the space charge layer and thickness of the space charge layer in VOCs gases, and led to increase in resistance and therefore response.

### 1. Introduction

With the development of the world's economy, environmental issues become the subject of widespread concern. Recently, an indoor air pollutant detection and environmental evaluation have attracted more and more attention. Volatile organic

compound vapors (VOCs), such as isopropanol, acetone, ethanol, formaldehyde, and so on, are the primary sources of indoor environmental pollutants and are considered seriously harmful to the human body.<sup>1</sup> For example, formaldehyde (HCHO) is one of the most harmful gases among indoor air pollutants, which has been proven to be a human carcinogen and an allergen, and can cause dermatitis, respiratory irritation, asthma, and pulmonary edema.<sup>2,3</sup> Its toxicity is similar with methanol, ethanol, isopropanol and acetone, which are classified as dangerous substances. Therefore, effective methods to monitor volatile organic compound (VOC) vapors have been demanded for atmospheric environmental measurements and control. Up to now, several methods, such as spectroscopic, electrochemical, chemiluminescent, and conductive polymer sensor methods have been developed for the detection of VOCs.<sup>4–9</sup> Colorimetric detection offers a cheap alternative method, but it is generally slow (typically 30 min) and inaccurate. However, most of these methods have several limitations and disadvantages such as their large size, high cost, complex fabrication process, slow response, and unreliability, so there is a need to develop inexpensive and maintenance-free VOCs gas sensors. As typical semiconductor metal oxide novel sensing devices, chemical microsensors (chemical sensors based on tiny changes in resistance

<sup>a</sup>School of Physics Science and Technology, Yunnan University 650091, Kunming, People's Republic of China; Fax: +86-871-65153832; Tel: +86-871-65031124; E-mail: ydwang@ynu.edu.cn.

<sup>b</sup>Yunnan Province Key Lab of Micro-Nano Materials and Technology, Yunnan University 650091, Kunming, People's Republic of China.

<sup>c</sup>Ruder Bošković Institute, Bijenička 54, 10000 Zagreb, Croatia; Fax: +38514680114; Tel: +38514680113; E-mail: igor.djerdj@irb.hr.

Electronic Supplementary Information (ESI) available: [Sketch of the structure of a typical NiO hollow microspheres gas sensor and photograph of the gas sensor (Fig. S1), schematic diagram of testing principle for NiO hollow microspheres gas sensor (Fig. S2), Fig. S3 Nitrogen adsorption/desorption isotherms for the samples of NiO hollow microspheres, structural data and refinement parameters for NiO hollow microspheres calculated by Rietveld refinement (Table S1) and comparison of varied nickel oxide nanostructures in VOCs sensing performances (Table S2), Fig. S4 (a), (b), (c), (d) and (e) are the isopropanol, acetone, methanol, ethanol and formaldehyde featured response and recovery characteristic curve versus time, Fig. S5 (a), (b), (c), (d) and (e) are the reproducibility of NiO hollow microspheres to VOCs (isopropanol, acetone, methanol, ethanol and formaldehyde) with a concentration of 50 ppm by 5 cycles, respectively.]. See DOI: 10.1039/x0xx00000x

response to the binding of analyses) are considered to be leading candidates due to their advantages such as low power consumption, exquisite sensitivity and fast response to the surrounding environment.<sup>10-12</sup> Gas sensors with nanostructured semiconducting metal oxides is thought to be a desirable means for monitoring VOCs.

The gas sensing process of metal oxide sensors generally involves a catalytic reaction between the gas to be monitored and the adsorbed oxygen on the surface of the sensor. In view of the sensing mechanism, the particle size, defects, surface, interface properties, and stoichiometry directly affect the state and the amount of oxygen species on the surface of the sensors, and consequently the performance of metal oxide-based sensors. The preparation method for the sensing material therefore plays an important role in tailoring the morphological characteristics of the sensor. In recent years, nanostructured materials have received a tremendous amount of attention because of their unique properties derived from the size, shape, orientation, and a high surface area. Because of the high surface-to-volume ratio and high surface activity, nanostructured metal oxides exhibited superior performance for gas sensors. As an important member of the p-type semiconductor oxide for gas sensors, nickel oxide (NiO) has attracted extensive investigation due to its significant qualities such as the relative wide band gap ( $E_g=3.6-4.0$  eV), relatively considerable electrical conductivity change along with chemical reactions on the surface of materials, etc., all making it a good candidate for the gas sensor application. Much effort has been focused on dimension and shape control of NiO in order to provide a large surface area and allow for good accessibility. Over the past several years, various morphologies of nanoscale NiO such as nanoparticles,<sup>13-15</sup> nanoplates,<sup>16,17</sup> hexagonal nanodisks,<sup>18</sup> nanotubes,<sup>19,20</sup> nanowires,<sup>21-24</sup> concave polyhedrons,<sup>25</sup> nanowalls,<sup>26</sup> nanoblocks,<sup>23</sup> nanosheets,<sup>24,27</sup> nanorods,<sup>23</sup> have been successfully synthesized and their gas sensing properties have been investigated. As far as NiO hollow spheres have been successfully prepared by using such as hydrothermal synthesis,<sup>28</sup> solvothermal synthesis,<sup>29</sup> chemical precipitation.<sup>30</sup> Gas sensing properties of NiO hollow microspheres have been studied, too. NiO hollow microspheres reported previously in literature were prepared by the  $\text{Ni}(\text{HCO}_3)_2$  precursor,<sup>31</sup> or by oxidation coatings of Ni precursors onto Ni spheres and subsequent removal of core Ni,<sup>32</sup> or polymeric colloidal templating method.<sup>33</sup> However, these nanostructured NiO, including NiO hollow microspheres, show very poor gas sensing properties for VOCs. It is essential to enhance the gas response of NiO in order to use it in practical sensor applications. Therefore, high sensing NiO material for the detection of VOCs gases is still to be developed.

In this paper, NiO hollow microspheres with a high surface area were obtained by a simple water bath method using  $\text{Ni}(\text{NO}_3)_2 \cdot 6\text{H}_2\text{O}$  and  $\text{CO}(\text{NH}_2)_2$  as precursors,  $\text{SiO}_2$  microsphere as template. The promising sensing properties for VOCs gases are reported.

## 2. Experimental

### 2.1. Preparation of NiO hollow microspheres

All the chemical reagents used in the experiments were obtained from commercial sources as guaranteed-grade reagents and used without further purification.  $\text{SiO}_2$  microspheres were prepared by base hydrolysis and condensation of tetraethyl orthosilicate in an aqueous ethanol medium containing ammonia.<sup>34</sup> Typically, 4.8 ml  $\text{NH}_4\text{OH}$  (25%, A.R.) and 20 ml deionized water were added into 63 ml absolute ethanol and strongly stirred at room temperature until a homogenous solution was obtained. Twelve milliliter tetraethoxysilane was introduced into the mixed solution with stirring for 0.5 h, resulting in the formation of white silica colloidal suspension. After diluting with ethanol and ultrasonic irradiation for 3 min, the product was aged at room temperature for 4 days. The resulting suspension was filtered, washed with deionized water, dried at ambient temperature. NiO hollow microspheres were synthesized by water bath method using  $\text{SiO}_2$  microsphere as template, the simple chemical materials ( $\text{Ni}(\text{NO}_3)_2 \cdot 6\text{H}_2\text{O}$  and  $\text{CO}(\text{NH}_2)_2$ ), as inorganic precursor and counterions, respectively. Reactions were performed in constant temperature water bath bath at 85 °C. The synthetic procedure was as follows: (1) The obtained  $\text{SiO}_2$  microsphere are dispersed into 60 ml of ethanol and sonicated for 2 h to reach good dispersion; (2) The  $\text{Ni}(\text{NO}_3)_2 \cdot 6\text{H}_2\text{O}$  and the urea are dissolved into 100 ml of deionized water with stirring until a green transparent solution was obtained; (3) The above two solutions are then mixed and heated to 85 °C in a water bath for 12 h. The molar ratio of  $\text{Ni}(\text{NO}_3)_2 \cdot 6\text{H}_2\text{O}:\text{CO}(\text{NH}_2)_2:\text{SiO}_2$  was 1:12:2. After the solution is cooled down to room temperature naturally, the product is collected through centrifugation and washed with deionized water and ethanol for several times. The products are then dried, followed by annealing at 450 °C for 4 h with a slow heating rate of 1 °C  $\text{min}^{-1}$  in order to get well defined crystallized NiO@ $\text{SiO}_2$  composites. Then products soaked in 1 M NaOH solution overnight to remove  $\text{SiO}_2$  template. After centrifugation, the products were washed with deionized water for several times and then dried to get pure NiO hollow microspheres.

### 2.2. Structural characterization

Powder X-ray diffraction (XRD) data were carried out by Rigaku D/max-3B diffractometer with an incident X-ray wavelength of 1.5406 Å (CuK $\alpha$  line), operated at 40 kV, 200 mA. The sample was scanned from 10° to 90° ( $2\theta$ ) in steps of 0.01°. Scanning electron microscopy (SEM) analysis was performed by means of FEI QUANTA200 with microscope operating at 30 kV. The samples for SEM were prepared by dispersing the final powders in the conductive glue; this dispersing was then sprayed with gold. Detailed studies of the microstructure were also carried out by transmission electron microscopy (TEM) and high-resolution transmission electron microscope (HRTEM) (JEOL JEM-2100) at an acceleration voltage of 200 kV.

### 2.3. Sensing device fabrication and measurement

In order to prepare series of sensors, we elected the indirect-heating structure (Fig. S1 in ESI). The sensor was prepared by coating as-prepared NiO hollow microspheres dispersed in water as a sensing layer with a thickness of about 0.6-0.8 mm on a prefabricated alumina tube (7 mm in length and 1.5 mm in diameter) with gold electrodes and platinum wires. The element was calcined at 400 °C for 2 h. A Ni-Cr heating wire was inserted into the tube to provide the working temperature for the gas sensors. In order to improve the stability and repeatability of the sensors, the fabricated sensors were aged at 300 °C for 7 days in a

Measurements on the gas sensing properties of the sensor were performed on a WS-30A system (Weisheng Instruments Co. Zhengzhou, China), which uses a conventional circuit (Fig. S2 in ESI) in which the element was connected with an external resistor in series at a circuit voltage of 5V. A certain volume of target gas was injected into the test chamber by a micro-injector and mixed with air (the relative humidity was below 30%) by two fans in the test chamber, and clean air was used as a reference gas. The operating temperatures of the sensor are ranging from 200 to 300 °C. The electrical response of the sensor was measured with an automatic test system, controlled by a personal computer.

### 3. Results and discussion

The phase purities of the products were examined by X-ray diffraction (XRD) measurement. In addition, the initial assignment was further confirmed by the refinement of the diffraction patterns with the Rietveld method.<sup>35</sup> Fig. 1 shows the experimental X-ray diffraction patterns, together with the calculated patterns obtained from the Rietveld refinement and the difference profile of the sample. As shown in Fig. 1, all diffraction peaks can be perfectly indexed to a pure cubic phase (space group: Fm-3m (225)) of NiO with lattice constants  $a = 4.177 \text{ \AA}$  (JCPDS No. 47-1049). The  $hkl$  indices indicated in the plot correspond to the NiO spinel structure. No crystalline by-products such as SiO<sub>2</sub>, Ni(NO<sub>3</sub>)<sub>2</sub>·6H<sub>2</sub>O or other nickel oxides are found in the patterns, indicating that the as-synthesized samples are pure NiO. The relative intensities of (200) peak are the largest. This is a common phenomenon in the growth of the nanostructures along their direction of growth. The other structural parameters obtained from the Rietveld profile refinement are presented in Table S1 in ESI. The calculated values are in good agreement with the experimental XRD patterns.

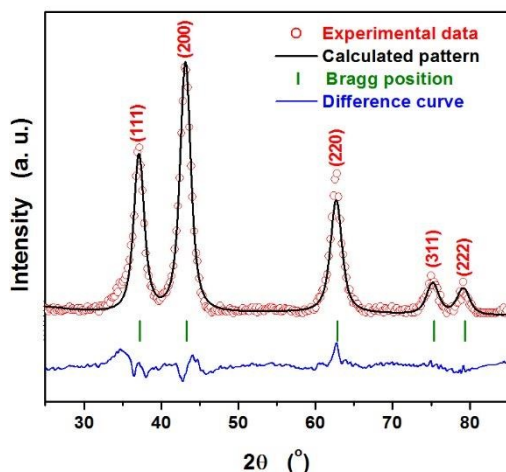


Fig. 1 X-ray diffraction pattern of NiO hollow microspheres.

SEM micrograph and microstructure of the resulting products are given in Fig. 2. The low magnification image (Fig. 2(c)) reveals that the samples consist of a large number of hollow spheres with the diameters about 350-400 nm. One can see that the surfaces of the NiO microspheres have small holes (as shown in Fig. 2(d)). It seems that the microspheres are loose and porous, which would relate to the release of water and carbon dioxide during the thermal treatment process. All these observations suggest the successful formation of NiO hollow microspheres by water bath method.

The morphologies of the nanostructured SiO<sub>2</sub>@NiO core-shell composite nanospheres and of the hollow microspheres of NiO nanosheets, prepared as discussed above, are characterized by electron microscopy (TEM) and high resolution transmission electron microscopy (HRTEM), the results are shown in Fig. 3. The TEM image displayed in Fig. 3(a) and (b) clearly show the SiO<sub>2</sub>@NiO core-shell composites, the SiO<sub>2</sub> spheres are covered ultrathin NiO nanosheets that are randomly oriented, creating a spherical shell of large porosity. By soaking with NaOH solution, the SiO<sub>2</sub> spheres are removed, get pure NiO hollow microspheres. The NiO spheres show interior hollow structure, meaning that the shell layer of the sphere consists of cross-linked nanoflakes (Fig. 3(c) and (d)). The image also demonstrates that the nanosheets are very thin, with typical thickness in the range of 20 nm to 40 nm. It is obviously thought that this kind of hollow nanostructures is instrumental in increasing the contact area of NiO with the electrolyte, thereby permitting faster transport of electrolyte ions. HRTEM images of NiO hollow spheres shown in Fig. 3(e) indicates that the nanostructures are structurally uniform with an interplanar spacing of about 0.211 nm, which corresponds to the (200) plane of cubic NiO. In fact, SAED patterns of NiO can be indexed as the cubic structure without any detectable secondary phase, which well interpret the intensified peaks in XRD pattern. The selected area electron diffraction (SAED) patterns shown in Fig. 3(f) indicate these hollow spheres are polycrystalline. The results agree well with the XRD patterns.

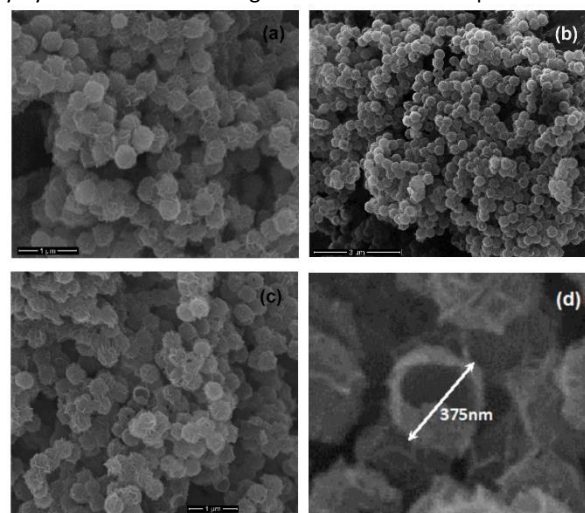
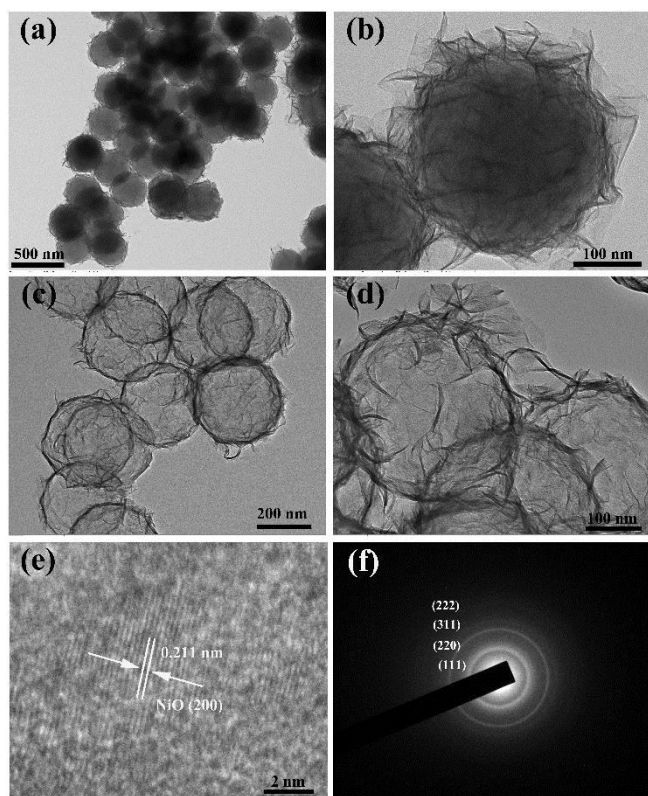


Fig. 2 SEM images of NiO coated SiO<sub>2</sub> microspheres (a) and the overall and typical hollow NiO<sub>2</sub> microspheres at the different magnifications (b), (c) and (d).

Fig. 4 illustrates the major process steps in this study. Firstly, the SiO<sub>2</sub> microsphere as a template, added Ni<sup>2+</sup> ions in Ni(NO<sub>3</sub>)<sub>2</sub> solution through ultrasonic dispersion. Secondly, urea was added in above solution and hydrolyzed to slowly release NH<sub>3</sub> and CO<sub>2</sub> under water bath at 85 °C for 12 h. Then the NH<sub>3</sub> and CO<sub>2</sub> reacted with Ni<sup>2+</sup> ions to generate Ni<sub>2</sub>(OH)<sub>2</sub>CO<sub>3</sub>. After calcining at 450 °C for 4 h with a slow heating rate of 1 °C min<sup>-1</sup> to get well defined crystallized NiO@SiO<sub>2</sub> composites. In order to remove the SiO<sub>2</sub> microsphere template, we use NaOH solution soaking overnight. Finally, the pure NiO hollow microspheres were obtained.

The optimal molar ratio of Ni(NO<sub>3</sub>)<sub>2</sub>·6H<sub>2</sub>O:CO(NH<sub>2</sub>)<sub>2</sub>:SiO<sub>2</sub> was 1:12.5 to form NiO hollow microspheres. If the ration of Ni(NO<sub>3</sub>)<sub>2</sub>·6H<sub>2</sub>O:CO(NH<sub>2</sub>)<sub>2</sub>:SiO<sub>2</sub> is more than 1:12.5, the as-prepared sample will have NiO nanosheets, which can not be assembled into hollow microspheres. On the other hand, the ration of





**Fig. 3** (a) and (b) are TEM micrograph of the SiO<sub>2</sub>@NiO core-shell composites, (c), (d), (e) and (f) are the Low-magnification, High-magnification TEM micrograph and the selected area electron diffraction pattern (SAED) of NiO hollow microspheres.

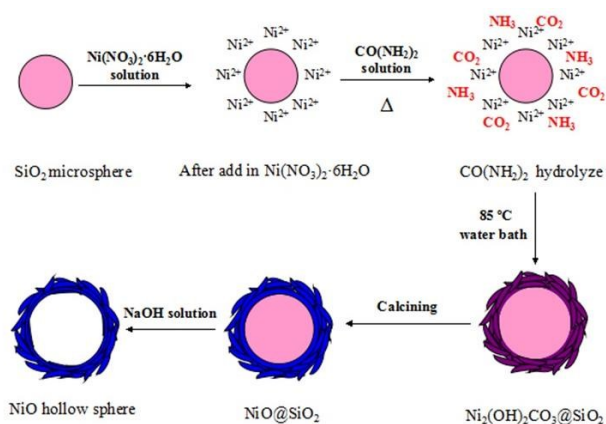


**Fig. 4** Schematic presentation of the formation mechanism of NiO hollow microspheres

Ni(NO<sub>3</sub>)<sub>2</sub>·6H<sub>2</sub>O:CO(NH<sub>2</sub>)<sub>2</sub>:SiO<sub>2</sub> is less than 1:12:2, hollow microspheres will be not formed.

According to the nitrogen adsorption/desorption isotherms (Fig. S3) for the sample of NiO hollow microspheres, the surface area of NiO microspheres is 167.31 m<sup>2</sup>/g, which is higher than the values reported in the previous work for NiO structures.<sup>15,20,21,23,27,32</sup> the surface area of NiO microspheres is more than other NiO structures, such as NiO nanosheet (65.6 m<sup>2</sup>/g),<sup>27</sup> NiO nanoparticles (127 m<sup>2</sup>/g),<sup>15</sup> NiO nanowires (136.1 m<sup>2</sup>/g),<sup>21</sup> NiO nanoblocks (20.4 m<sup>2</sup>/g),<sup>21</sup> NiO nanorods (86.8 m<sup>2</sup>/g),<sup>23</sup> NiO porous nanotube (161.6 m<sup>2</sup>/g),<sup>20</sup> and NiO hollow microspheres (11.2 m<sup>2</sup>/g).<sup>32</sup>

The calcine conditions are important to form NiO hollow microspheres. If the temperature or heating rate too big, hollow structure will collapse, and the surface area will decrease. According to the experimental data, calcine conditions of annealing at 450 °C for 4 h with a slow heating rate of 1 °C min<sup>-1</sup> are the optimal conditions to obtain NiO hollow microspheres.

In order to understand the role of NiO microspheres spheres and demonstrate the potential applications in highly sensitive and selective gas sensors, five VOC vapors including isopropanol, acetone, methanol, ethanol and formaldehyde have been measured, respectively. The operating temperature is one of the most important factors for the gas sensor, which highly determined the nature of the materials itself and the gas-sensing process of the gas towards the surface of materials. So the first step to be studied is the optimal operating temperature. Fig. 5 represents the typical relationship between gas response and operating temperature of NiO hollow spheres sensor for ethanol with a concentration of 50 ppm. Interestingly, the response first increases gradually and then decreases with increasing the operating temperature. As shown in Fig. 5, the best operating temperature for methanol and formaldehyde is at 220 °C. It is attributed to the amount of adsorbed VOCs increases when the operating temperature becomes high and adsorption attains a balance at a suitable temperature (namely optimum operating temperature), because adsorption is an exothermic reaction.<sup>36</sup> When the operating temperature keeps on increasing, the amount of gas adsorbed will reduce, resulting in decreased gas sensitivity when the operating temperature surpasses the optimum values.<sup>37</sup> The NiO hollow spheres based sensor shows responses of approximately 6.0, 7.5, 5.4, 4.1, 3.1, 2.7 at 200 °C, 220 °C, 240 °C, 260 °C, 280 °C, 300 °C in ethanol with a concentration of 50 ppm. It indicates that the NiO hollow spheres have high sensitivity in low concentration VOCs.

The sensing responses as an R<sub>gas</sub>/R<sub>air</sub> function of gas concentrations from 50 ppm to 600 ppm for five tested gases at an operating temperature of 220 °C are summarily plotted in Fig. 6. It is apparent that the response of all sensors increases along with increasing VOCs (isopropanol, acetone, methanol, ethanol and formaldehyde) gas concentrations. The response of NiO hollow microspheres based sensor was linear from 5 to 600 ppm. At the measured temperature, the sensor resistance increases upon exposure to VOCs (isopropanol, acetone, methanol, ethanol and formaldehyde) recover approximately to the initial value when the test chamber is refreshed with air, which is expected for a p-type semiconductor upon exposure to reducing gas.<sup>38</sup> A good response and quick response/recovery time were observed with NiO hollow microsphere sensor at an optimal operating temperature of 220 °C (Figure S3 and Figure S4). As important parameters for tailoring a sensor for practical applications, the response time calculated from the case of 50 ppm (defined as the time required to reach 90% of the final equilibrium value) of NiO hollow microsphere based sensor in VOC (isopropanol, acetone, methanol, ethanol and formaldehyde) gas is 40 s, 60 s, 65 s, 82 s and 120 s, while the recovery time calculated from the case of 600 ppm is 105 s, 126 s, 168 s, 189 s and 206 s.

Table S2 compares the sensing performance of NiO hollow microspheres against previously reported nickel oxide nanostructures in VOCs sensing performances. Operating temperature is generally high reported in literatures, but operating temperature of the sensor based on NiO hollow microspheres is only 220 °C in this work, moreover, the responses are several times higher than those reported in literatures.

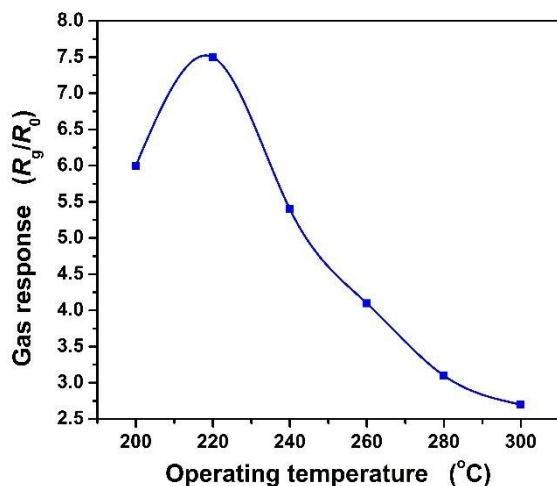


Fig. 5 The typical relationship between gas response and operating temperature of NiO hollow microspheres sensor for ethanol with a concentration of 50 ppm.

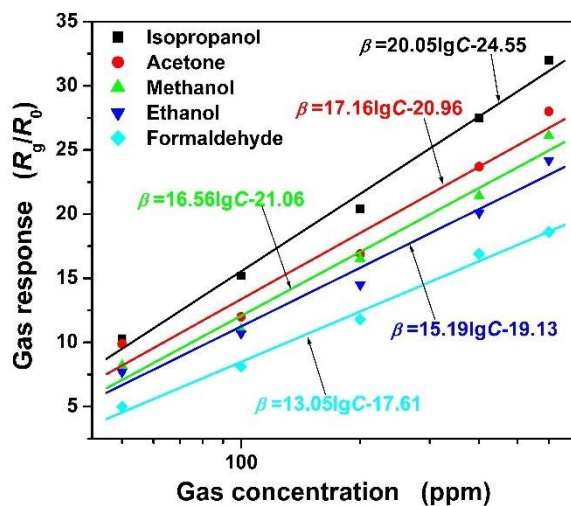


Fig. 6 The response versus VOCs (isopropanol, acetone, methanol, ethanol and formaldehyde) gases concentrations at operating temperature of 220 °C.

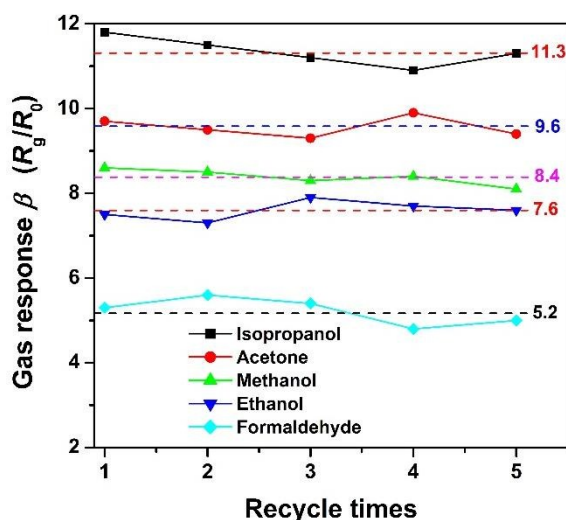


Fig. 7 The reproducibility of NiO hollow microspheres to VOCs with a concentration of 50 ppm by 5 cycles at operating temperature of 220 °C, respectively.

To verify the repeatability of the sensor, the gas response evolutions in about 5 cycles were tested under different VOC gas with a concentration of 50 ppm. Fig. 7 illustrates the reproducibility of the NiO hollow microspheres based sensor, revealing that the sensor maintains its initial response amplitude without a clear decrease upon 5 cycles successive sensing tests 50 ppm of VOCs (isopropanol, acetone, methanol, ethanol and formaldehyde). From the Fig. 7, we can see NiO hollow spheres based sensor has good stability in these VOCs gas.

In practical applications, the long-term stability of gas sensors has attracted much attention for which the reliability of gas sensors and the length of service were determined. To verify the stability of the sensor, the gas response evolutions in about 2 weeks were tested for the different VOCs gases (50 ppm isopropanol, acetone, methanol, ethanol and formaldehyde). The 14-days-later response is slightly changed  $\pm 3.4\%$ ,  $\pm 2.6\%$ ,  $\pm 4.3\%$ ,  $\pm 3.3\%$  and  $\pm 6.9\%$  for isopropanol, acetone, methanol, ethanol and formaldehyde gas, respectively, illustrating good stability of the sensor (Fig. 8). The stability mechanism is more complicated and further work is to be done to get a definite understanding.

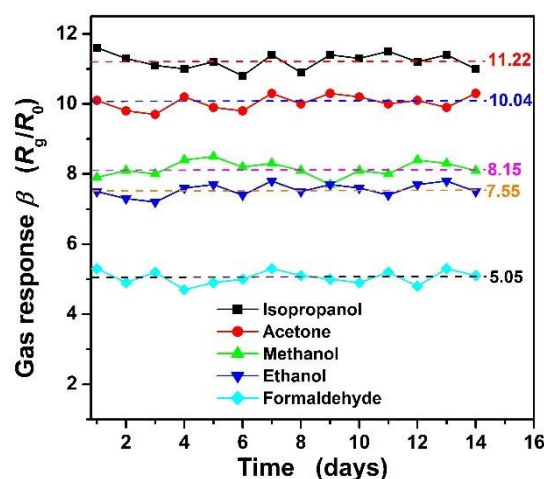
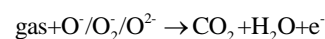


Fig. 8. The gas response of NiO hollow microspheres to 50 ppm VOCs gases tested once a day for up to 14 days at operating temperature of 220 °C.

Sensing device measurement was carried out at the relative humidity of 30%. Our experimental data show that the humidity effect on the sensor is small. When the relative humidity less than 50%. When the humidity is more than 50%, the response of sensor to VOCs will slightly decrease.

The gas sensing properties in the oxide-based sensing materials are mainly governed via surface reactions and the effective diffusion of target gases. Thus, the sensitivity of gas sensors is greatly affected by morphology and the nature of the sensor materials. Previous studies related the oxygen adsorption over NiO surface suggested that  $O^-$  is dominating up to 150–200 °C. Above 200 °C,  $O^{2-}$  is the main species.<sup>39</sup>

Therefore, the absorbed oxygen could be a great number of  $O^{-2}$ ,  $O^-$ ,  $O^{2-}$  determined by the activation energies on the surface of NiO.<sup>14,40</sup> The sensing process of the target gases decomposition reaction on the surface of the NiO can be possibly expressed as following:



After exposure to the reducing gases, the adsorbed oxygen was consumed, leading to a decrease in the space charge layer and thickness of the space charge layer. The adsorbed oxygen acts as a sort of acceptor to target gas brought about a resistance change, thereby reflection the species and concentrations of tested gas. The responses to isopropanol ((CH<sub>3</sub>)<sub>2</sub>CHOH), acetone (C<sub>2</sub>H<sub>6</sub>CO), methanol (CH<sub>3</sub>OH), ethanol (C<sub>2</sub>H<sub>5</sub>OH), formaldehyde (CH<sub>2</sub>O) of the NiO hollow spheres sensors measured at 220 °C (Fig. 6) show that the sensor is more sensitive to isopropanol than to the other four gases. It is interesting that the response to isopropanol is 2 times higher than to formaldehyde, and the sensor is also sensitive to acetone, methanol, and ethanol. The gas responses of those five reductive gases of isopropanol, acetone, methanol, ethanol and formaldehyde at a concentration of 50 ppm are 11.3, 9.9, 8.2, 7.7 and 5.0, respectively, which is higher than previously literatures reported (Table S2).

The gas responses are 33.0, 28.0, 26.1, 24.2 and 18.6 at a concentration of 600 ppm for those five VOCs gases. The results show that the NiO hollow microspheres have a perfect sensing performance to VOCs gases. It is attributed to the NiO hollow microspheres offer a high surface-to-volume ratio and an intrinsically large specific surface area, leading to improved surface activities. This means that the NiO hollow microspheres have a perfect sensing performance to VOCs gases.

## Conclusions

In conclusion, the successful synthesis of NiO hollow microspheres by calcination Ni<sub>2</sub>(OH)<sub>2</sub>CO<sub>3</sub>@SiO<sub>2</sub> core-shell structures obtained by a water bath method using Ni(NO<sub>3</sub>)<sub>2</sub>·6H<sub>2</sub>O and CO(NH<sub>2</sub>)<sub>2</sub> as precursors, SiO<sub>2</sub> microspheres as template and then by soaking in NaOH solution to remove SiO<sub>2</sub> template is presented. The materials were structurally characterized by means of XRD, SEM and TEM in order to correlate physical properties with gas sensing behaviors. The NiO hollow microspheres can be used directly to prepare gas sensor devices by fabrication of the NiO hollow microspheres on the alumina tubes with Au electrodes and platinum wires. The fabricated sensor showed good response, quick responses and recovery, good selectivity, and good stability to VOCs (isopropanol, acetone, methanol, ethanol and formaldehyde) gas at an operating temperature of 220 °C. The gas responses at a concentration of 50 ppm are 5 times higher than previously literature reports which can be ascribed to high specific surface area of active material used in amounts of 167.31 m<sup>2</sup>/g. The results demonstrate that our produced sensor is a potential candidate as higher performance gas sensors.

## Acknowledgements

This work was supported by National Natural Science Foundation of China (Grant No.51262029), the Key Project of the Department of Education of Yunnan Province (ZD2013006), Program for Excellent Young Talents, Yunnan University, and Yunnan University Graduate Program for Research and Innovation (Grant No. ynuy201392). Igor Djerdj acknowledges financial support from the Unity through Knowledge Fund ([www.ukf.hr](http://www.ukf.hr)) of the Croatian Ministry of Science, Education and Sports (Grant Agreement No. 7/13),

and from the Croatian Center of Excellence for Advanced Materials and Sensing Devices.

## Notes and references

1. L. Francioso, A. Forleoa, A. M. Taurino, P. Siciliano, L. Lorenzelli and V. Guarnieri, *Sens. Actuators B*, 2008, **134**, 660.
2. M. Agathos and H. A. Bernecker, *Derm. Beruf. Umwelt.*, 1982, **30**, 43.
3. A. J. Hempel, K. S. Kjaergaard, L. Molhave and H. K. Hundnell, *Arch. Environ. Health*, 1999, **54**, 416.
4. G. J. Mohr, U. E. Spichiger, W. Jona and H. Langhals, *Anal. Chem.*, 2000, **72**, 1084.
5. Y. Suzuki, N. Nakano and K. Suzuki, *Environ. Sci. Technol.*, 2003, **37**, 5695.
6. J. R. Nicole and V. D. Serger, *Sensors*, 2008, **8**, 2569.
7. L. Feng, C. J. Musto and K. S. Suslick, *J. Am. Chem. Soc.*, 2010, **132**, 4046.
8. Y. Liu, S. Antwi-Boampong, J. J. BelBruno, M. A. Crane and S. E. Tanski, *Nicotine Tob Res.* 2013, **15**, 1511.
9. H. Bai and G. Q. Shi, *Sensors* 2007, **7**, 267.
10. F. Wang, H. W. Gu and T. M. Swager, *J. Am. Chem. Soc.*, 2000, **130**, 5392.
11. L. T. Kong, J. Wang, X. C. Fu, Y. Zhong, F. L. Meng, T. Luo and J. H. Liu, *Carbon*, 2010, **48**, 1262.
12. P. C. Chen, S. Sukcharoenchoke, K. Ryu, L. G. Arco, A. Badmaev, C. Wang and C. W. Zhou, *Adv. Mater.*, 2010, **22**, 1900.
13. X. L. Zhang, F. Z. Huang, A. Nattestad, K. Wang, D. C. Fu, A. Mishra, P. Bcauerle, U. Bach and Y. B. Cheng, *Chem. Commun.*, 2011, **47**, 4808.
13. G. X. Zhu, C. Y. Xi, H. Xu, D. Zheng, Y. J. Liu, X. Xu and X. P. Shen, *RSC Adv.*, 2012, **2**, 4236.
15. Y. Du, W. M. Wang, X. W. Li, J. Zhao, J. M. Ma, Y. P. Liu and G. Y. Lu, *Mater. Lett.*, 2012, **68**, 168.
16. Y. G. Li, B. Tan and Y. Y. Wu, *Chem. Mater.*, 2008, **20**, 567.
17. G. X. Zhu, H. Xu, Y. J. Liu, C. Y. Xi, J. Yang, X. P. Shen, J. Zhu and L. Yang, *J. Colloid Interface Sci.*, 2013, **412**, 100.
18. Z. Zheng, L. Huang, Y. Zhou, X. W. Hu and X. M. Ni, *Solid State Sci.*, 2009, **11**, 1439.
19. Y. Ren, W. K. Chim, S. Y. Chiam, J. Q. Huang, C. Pi and J. S. Pan, *Adv. Funct. Mater.*, 2010, **20**, 3336.
20. X. F. Song, L. Gao and S. Mathur, *J. Phys. Chem. C* 2011, **115**, 21730.
21. B. Liu, H. Q. Yang, H. Zhao, L. J. An, L. H. Zhang, R. Y. Shi, L. Wang, L. Bao and Y. Chen, *Sens. Actuators B*, 2011, **156**, 251.
22. W. Zeng, B. Miao, L. Y. Lin and J. Y. Xie, *Trans. Nonferrous Met. Soc. China*, 2012, **22**, s100.
23. B. Miao, W. Zeng, L. Y. Lin and S. Xu, *Physica E*, 2013, **52**, 40.
24. L. Y. Lin, T. M. Liu, B. Miao and W. Zeng, *Mater. Res. Bull.*, 2013, **48**, 449.
25. W. Zhou, M. Yao, L. Guo, Y. M. Li, J. H. Li and S. H. Yang, *J. Am. Chem. Soc.*, 2009, **131**, 2959.
26. K. L. Zhang, C. Rossi, P. Alphonse and C. Tenailleau, *Nanotechnology*, 2008, **19**, 155605.
27. G. H. Li, X. W. Wang, H. Y. Ding and T. Zhang, *RSC Adv.*, 2012, **2**, 13018.
28. Y. Wang, Q. S. Zhu and H. G. Zhang, *Chem. Commun.*, 2005, 5231.
29. T. Zhu, J. S. Chen and X. W. Lou, *J. Phys. Chem. C*, 2012, **116**, 6873.
30. S. M. Zhang and H. C. Zeng, *Chem. Mater.*, 2009, **21**, 871.



31. C. Y. Cao, W. Guo, Z. M. Cui, W. G. Song and W. Cai, *J. Mater. Chem.*, 2011, **21**, 3204.
32. H. J. Kim, K. I. Choi, K. M. Kim, C. W. Na and J. H. Lee, *Sens. Actuators B*, 2012, **171–172**, 1029.
33. N. G. Cho, I. S. Hwang, H. G. Kim, J. H. Lee and I. D. Kim, *Sens. Actuator B*, 2011, **155**, 366.
34. W. Stober, A. Fink and E. Bohn, *J. Colloid Interface Sci.* 1968, **26**, 62.
35. L. B. McCusker, R. B. Von Dreele, D. E. Cox, D. Louer and P. Scardi, *J. Appl. Crystallogr.* 1999, **32**, 36.
36. W. Wen, J. M. Wu and Y. D. Wang, *Sens. Actuators B*, 2013, **184**, 78.
37. W. Zeng and T. M. Liu, *Physica B*, 2010, **405**, 1345.
38. T. He, D. Chen, X. Jiao, Y. Wang and Y. Duan, *Chem. Mater.*, 2005, **17**, 4023.
39. A. Bielański and M. Najbar, *J. Catal.*, 1972, **25**, 398.
40. J. C. Fu, C. H. Zhao, J. L. Zhang, Y. Peng and E. Q. Xie, *ACS Appl. Mater. Interfaces*, 2013, **5**, 7410.